JOINT EUROPEAN TORUS JET

JET–P(87)37

The JET Team
(presented by R.J. Bickerton)

Operational Limits and Confinement in JET

Operational Limits and Confinement in JET

The JET Team
(presented by R.J. Bickerton)

JET-Joint Undertaking, Culham Science Centre, OX14 3DB, Abingdon, UK

Preprint of Paper to be submitted for publication in
Plasma Physics and Controlled Fusion

OPERATIONAL LIMITS & CONFINEMENT IN JET

The JET Team *

(Presented by R J Bickerton)

JET Joint Undertaking, Abingdon, Oxfordshire, OX14 3EA, UK

* See Appendix 1

ABSTRACT

Operational limits on JET in terms of density, current and plasma beta are described. The results for various heating schemes are displayed in the $\hat{n}\,\tau_E\,\hat{T}_i$ vs $\hat{T}_i$ plane against the contours of constant thermonuclear gain Q. The confinement data is compared with several scaling laws and the eventual performance of JET predicted. Finally the likelihood of ignition in the enhanced version of NET is assessed.

KEYWORDS

Tokamak; Fusion.

INTRODUCTION

JET is a large tokamak with the parameters listed in Table 1. It has been operated with plasma currents up to 5MA in limiter bounded mode and 3MA with a single null magnetic separatrix. The additional heating capability has been up to 10MW of neutral beam injection and 8MW of ion cyclotron resonance heating (ICRH). The machine has recently been modified in such a way that the above numbers will be increased to 7MA (limiter), 4MA (single null), 20MW (neutral beam) and 20MW (ICRH) respectively. A further modification planned for 1990 is the addition of 10MW of lower hybrid power for current drive studies.

In this paper we outline the operational limits already encountered together with the performance levels achieved. The theoretical MHD stability limits on β are then discussed and the existing experimental data presented. Several different scaling laws for the energy confinement time have been proposed on the basis of JET and other tokamak data. These are compared and the eventual JET performance is estimated. Scaling from the JET data the prospects for NET are considered.

TABLE 1

JET PARAMETERS

MAJOR RADIUS, R_o(m)	3.0
MINOR RADIUS OF PLASMA, a(m)	1.2
ELONGATION OF PLASMA CROSS-SECTION, K	≤1.8
TOROIDAL FIELD STRENGTH AT R_o, (T)	3.4
PLASMA CURRENT (MA)	
(a) LIMITER BOUNDED	5.0(7.0)
(b) SINGLE NULL X-POINT	3.0(4.0)
NEUTRAL BEAM HEATING POWER(MW)	10(20)
ICRF HEATING POWER (MW)	8(20)

(Bracketted figures are the anticipated performance levels for the 87/88 campaign.)

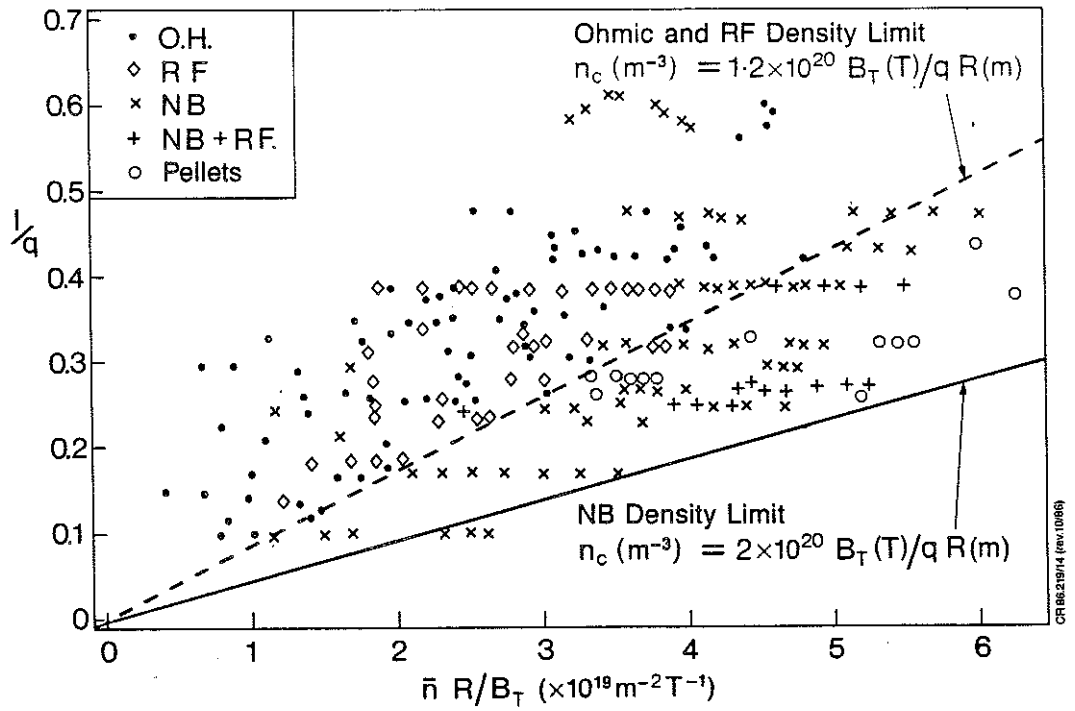

Fig. 1. Plot of operating conditions in normalised current, normalised density plane. $q_{CYL} = 5AB/\pi RI$ where A is the cross-sectional area of the plasma (m^2), B_T the toroidal field strength (T), R the major radius (m) and I the plasma current (MA). $\bar{n}$ is the average electron density (m^{-3}).

DENSITY AND CURRENT LIMITS

The density and current limits experienced on JET are presented in normalised form in Fig. 1.

Here q_{CYL} is defined as

$$q_{CYL} = \frac{5AB}{\pi RI}$$

where A is the cross-sectional area of the plasma, R the major radius, B the toroidal field strength and I the plasma current. Units are m, T, MA. The Murakami parameter M is defined as

$$M = \frac{\bar{n}R}{B}$$

where n is the average electron density in units of $10^{19}m^{-3}$.

The data in figure 1 shows that the operating regime is bounded on three sides. There is a working low density limit set approximately by $M<(1/q)$. This limit is complex and depends on the time history of the discharge. During the current rise phase the neutral particle influx and correspondingly the density must be above a minimum level to avoid MHD mode-locking and disruptions (J. Snipes et al, 1987) or the creation of runaway electrons with $\varepsilon>1$MeV. Once the flat-top in total current is reached the density can be progressively reduced by switching off gas input and moving the discharge on to a surface with a high particle pumping capacity such as the carbon tiles on the small major radius side of JET (referred to henceforth as the "inner wall"). In this way slide-away discharges can be created with densities down to $1.5\times10^{18}m^{-3}$ and with no sign of a lower limit other than the time available for pumping. Note that in the normalised plot, lines of constant ratio between $(1/q_{CYL})$ and M are lines of constant electron drift velocity, V_d

$$V_d = 1.6\times10^6\left(\frac{1}{Mq_{CYL}}\right)\ m/s$$

Another limiting line is the density limit above which the discharge disrupts. For normal Ohmic

and RF-heated discharges this is a fairly well defined boundary given by

$$(n_c)_1 = \frac{1.2\times10^{20}}{q_{CYL}}\frac{B}{R}$$

while with neutral beam injection at powers up to 10MW the limit is considerably higher at

$$(n_c)_2 = \frac{2\times10^{20}}{q_{CYL}}\frac{B}{R}$$

With ohmic heating alone the limit $(n_c)_1$ can be significantly exceeded by the injection of a single deuterium pellet.

A third line bounding stable operation is given by $1/q_{CYL} \sim 0.6$. Careful experiments have shown that this "low q" boundary is precisely given by $q_\Psi=2$, where q_Ψ is the actual field line safety factor at the plasma boundary. (Campbell et al, 1986)

Note that the achievable values of M in JET have a maximum at 6-7 for low q_{CYL} while the design value for NET is 16 (Engelmann, 1986) and for an economic reactor $\sim$ 30. Thus it is important to understand the mechanism of high density disruptions.

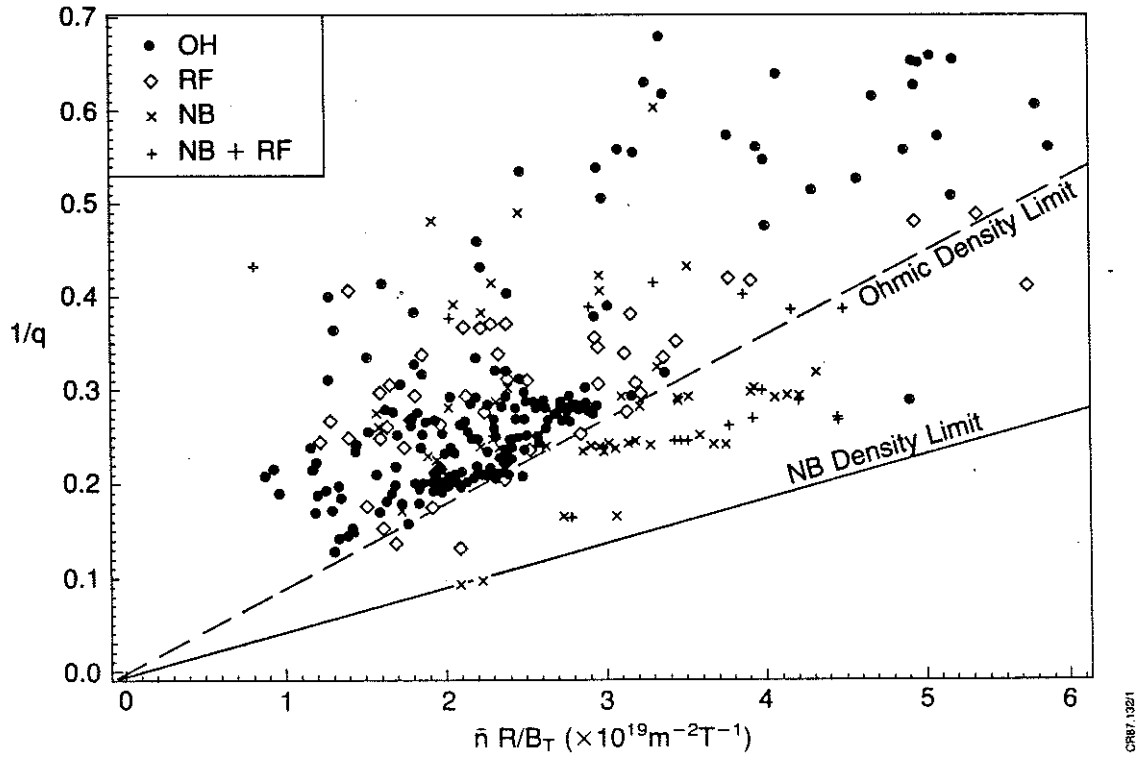

Fig. 2. Plot of operating conditions in the normalised current, ($1/_q$) normalised density ($\bar{n}R/B_T$) plane for the 1986 disruptions which occurred during the current flat-top.

Figure 2 shows the disruption data in the density-current plane for the flat-top phase of the plasma current waveform. Most of the points are well inside the so-called stable zone of Fig. 1. For $q_{CYL}>2.5$ these disruptions are nearly all preceded by a rise in the radiated power P_{RAD} to equal the input power. For $q_{CYL}<2.5$ the majority of the disruptions are not preceded by such a rise. These low q disruptions reflect the high sensitivity of discharges when the resonant surface $q_\Psi=2$ approaches the plasma boundary. In fact detailed study shows that high density disruptions are preceded by a rise in the radiated fraction followed by a shrinking of the temperature profile and of the current channel (Campbell et al, 1986). Thus some of the unpredictability of disruptions is related to varying contamination of the discharge. Increasing the power input into the discharge increases the density limit unless as in the RF case the increase in power is accompanied by an increase in the edge density. Deuterium pellet injection raises the density but reduces Z_{eff} while increasing the Ohmic input.

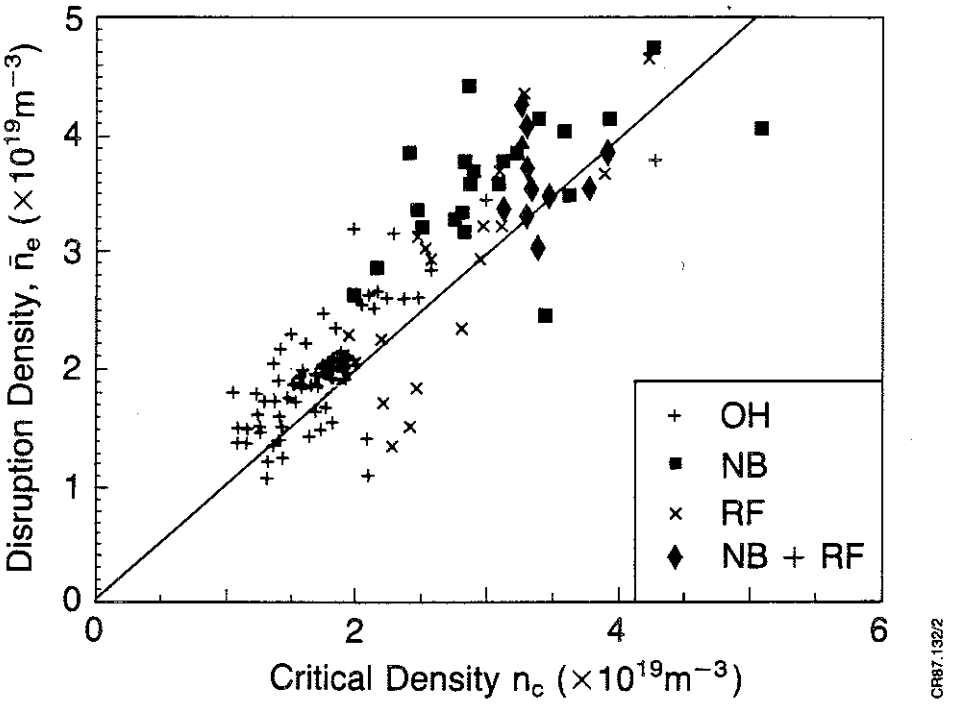

Fig. 3. Comparison between the density at disruption and the critical value predicted by the expression $n_c = 3.5 \left\{ \frac{P_{IN}\, q_{CYL}}{(Z_{eff}-1)\, R\, ab\, (q_{CYL}-2a/b)} \right\}^{1/4}$

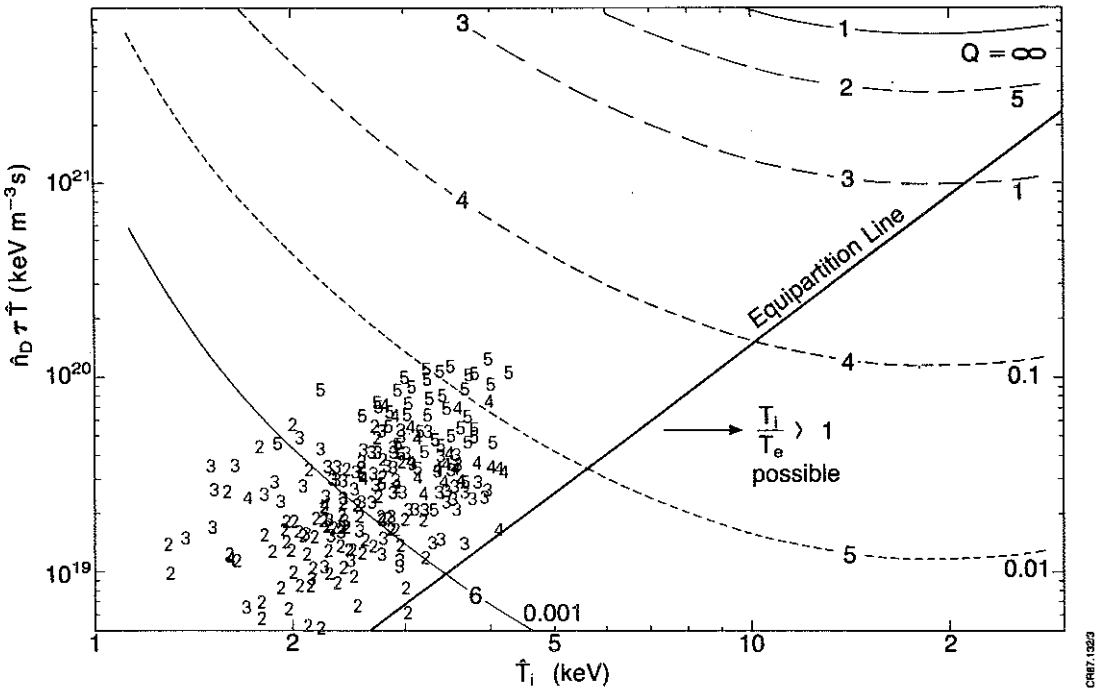

Fig. 4. Data for ohmic heating only discharges plotted in the $\hat{n}_D\, \tau_E\, \hat{T}_i - \hat{T}_i$ plane. Numbers refer to the current level in MA. Equipartition line shows $\hat{n}\, \tau_E\, \hat{T}_i = 4.5 \times 10^{17}\, \hat{T}_i^{5/2}$. Contours show lines of constant Q (Q=thermonuclear power output/power input). Discharges bounded by limiters or inner wall.

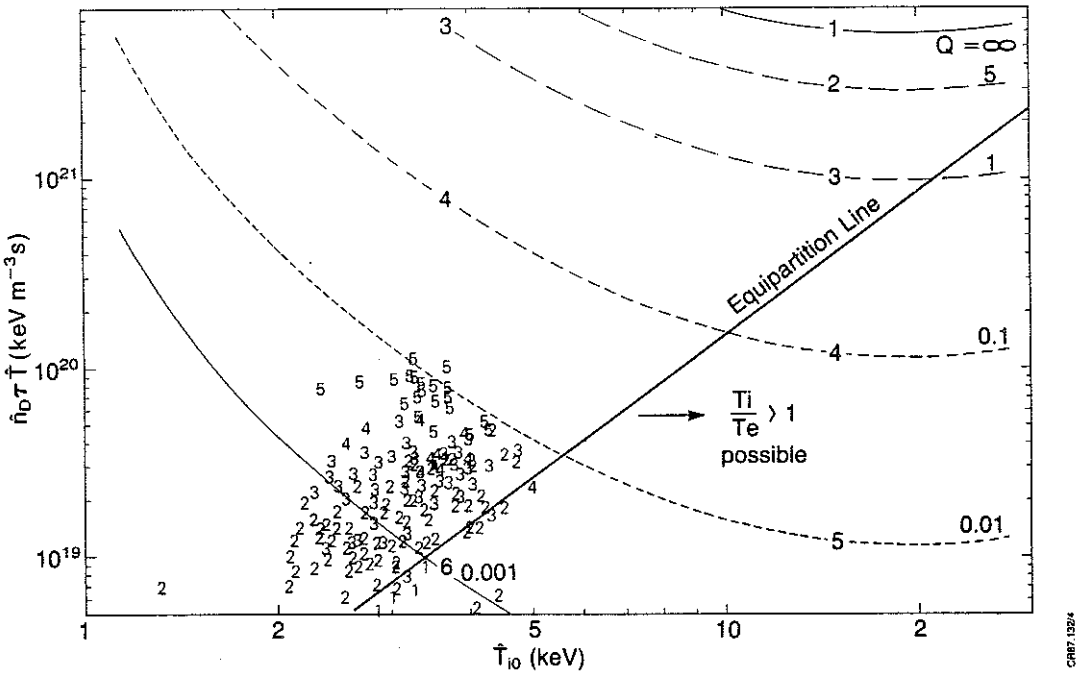

Fig. 5. Data for RF heating only discharges plotted in the $\hat{n}_D \tau_E \hat{T}_i - \hat{T}_i$ plane. Numbers refer to the current level in MA. Equipartition line shows $\hat{n} \tau_E \hat{T}_i = 4.5 \times 10^{17} \hat{T}_i^{5/2}$. Contours show lines of constant Q (Q=thermonuclear power output/power input). Discharges bounded by limiters or inner wall.

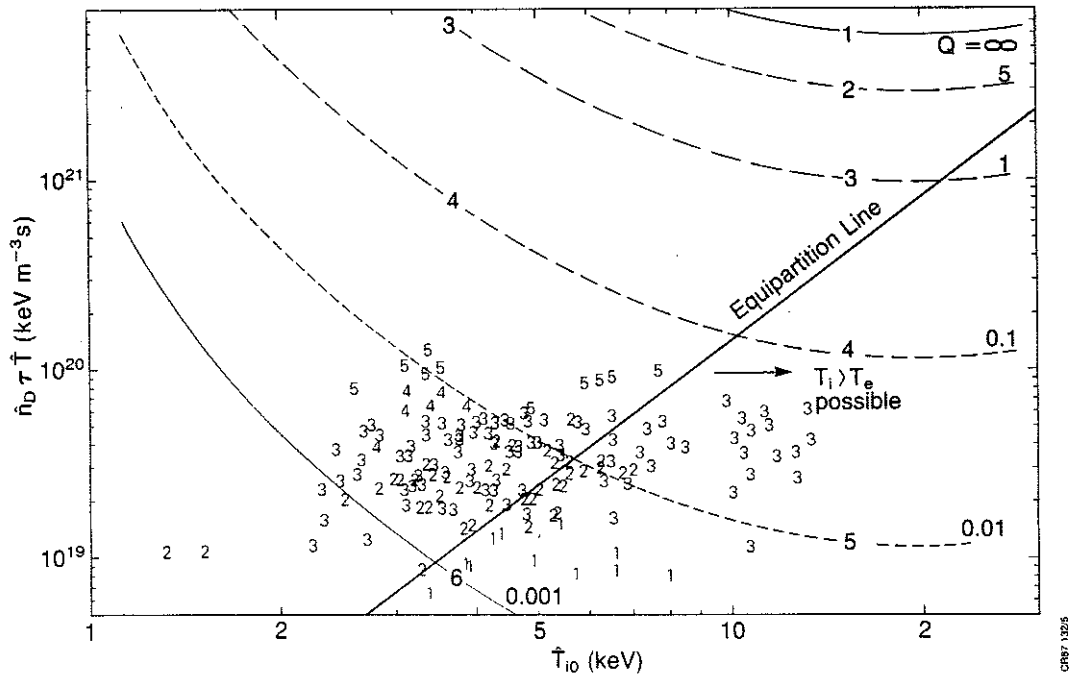

Fig. 6. Data for neutral beam heating only discharges plotted in the $\hat{n}_D \tau_E \hat{T}_i - \hat{T}_i$ plane. Numbers refer to the current level in MA. Equipartition line shows $\hat{n} \tau_E \hat{T}_i = 4.5 \times 10^{17} \hat{T}_i^{5/2}$. Contours show lines of constant Q (Q=thermonuclear power output/power input). Discharges bounded by limiters or inner wall.

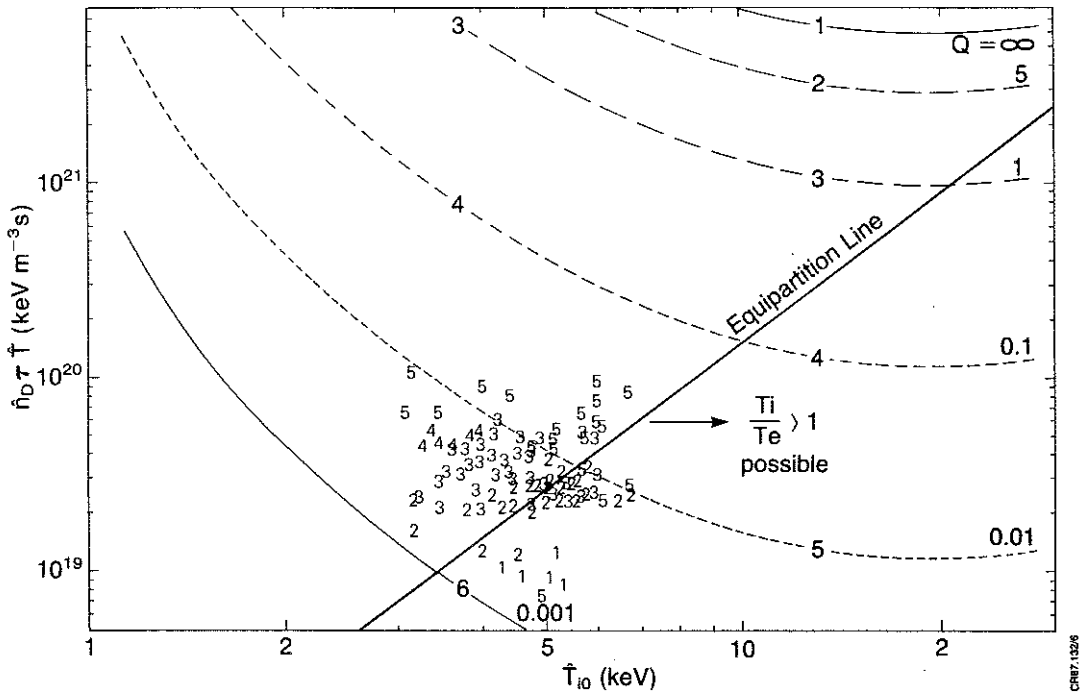

Fig. 7. Data for combined neutral beam and RF heating discharges plotted in the $\hat{n}_D \tau_E \hat{T}_i - \hat{T}_i$ plane. Numbers refer to the current level in MA. Equipartition line shows $\hat{n} \tau_E \hat{T}_i = 4.5 \times 10^{17} \hat{T}_i^{5/2}$. Contours show lines of constant Q (Q=thermonuclear power output/power input). Discharges bounded by limiters or inner wall.

A simplified model (Campbell et al, 1986) for low Z dominated discharges (ie valid for $Z_{eff} \neq 1$) based on the triggering of disruption as $P_{RAD}/P_{IN} \rightarrow 1$ gives

$$M = \frac{3.5}{B} \left\{ \frac{P_{IN} \; R \; q_{CYL}}{(Z_{eff}-1) \; a \; b \; (q_{CYL}-2a/b)} \right\}^{1/2}$$

where the units are m, MW and the term $\left(\frac{q_{CYL}}{q_{CYL} - 2a/b}\right)$ is approximately the ratio of the total volume to the volume outside the $q_\psi = 2$ surface.

This gives good agreement with JET data Fig. 3 and suggests that to achieve high M in future machines will require a substantial increase in the power input per unit length and a reduction of Z_{eff} compared with JET. This latter improvement is required in any case to reduce the depletion of the reacting fuel.

EQUIVALENT THERMONUCLEAR Q VALUES

Q is defined as, $\quad Q = \dfrac{P_{th}}{P_{input}}$

where P_{th} is the total thermonuclear output power for a D-T plasma.

$$P_{th} = \int dV \;\; n_D n_T \; (\overline{\sigma v}) \;\; Y$$

where $\overline{\sigma v}$ is the velocity cross-section product averaged over a Maxwellian ion distribution for temperature $T_i(r)$ and Y = 17.6MeV is the energy yield per reaction.

In steady state $\quad P_{INPUT} = P_{LOSS} - P_\alpha = P_{LOSS} - \dfrac{P_{th}}{5}$

where P_{LOSS} is the total power loss from the system and P_α is the α-power input which is assumed to be all deposited in the plasma.

$$P_{LOSS} = \frac{W}{\tau_E}$$

where W is the total energy content in the plasma and τ_E the global energy confinement time.

The JET results are plotted in the $\hat{n}\ \hat{T}_i\ \tau_E$ vs $\hat{T}_i$ plane in Figs. 4-7. In this plane are also plotted the contours of constant Q assuming $T_e=T_i$, the density and temperature profiles typical of the experiments and $n_D=n_T=\frac{1}{2}(n_D)_{Expt}$ where $(n_D)_{Expt}$ is the experimental deuteron density (determined from the measured Z_{eff} and the assumption that the depletion is due to carbon and oxygen).

The results for four different heating scenarios are shown in Figs. 4-7, namely for ohmic heating only, RF heating, neutral beam heating and combined RF and neutral beam heating. This data is for plasmas bounded on either the outer limiters or the inner wall. It is evident that the highest Q values (close to 0.1) are reached with 3MA discharges on the inner wall with neutral beam heating. The highest ion temperatures are reached in these same discharges where the strong pumping action of the carbon tiles enables the density to be kept low ($1\text{-}2\times10^{19}m^{-3}$). In these plasmas $T_i/T_e \sim 2$, giving the so-called hot ion mode. This means that the Q values derived from the contours are underestimated by a factor of $\frac{(1+T_e/T_i)}{2}$. The ability to increase the ratio T_i/T_e depends on two conditions,

(1) the additional heating system must predominantly heat the ions directly.
(2) the equipartition time τ_{equ} must be significantly longer than the global confinement time.

Classically

$$\tau_{equ} = \frac{0.084\ T_e^{3/2}\ (keV)}{n_{e19}}$$

If we define $T_i/T_e>1.5$ as a hot-ion mode then in the $\hat{n}\ \hat{T}_i\ \tau_e$ vs $\hat{T}_i$ plane the line

$$\hat{n}\ \tau_E\ \hat{T}_i = 4.5\times10^{17}\ \hat{T}_i^{5/2}$$

divides the regime where the hot ion mode is possible from that in which equipartion ensures $T_e \sim T_i$. This line is shown on Figs. 4-7 where we see that the neutral beam results at high ion temperature are all in the hot ion regime. Note that the hot ion mode criterion intersects the ignition requirement at $\hat{T}_i \sim 50keV$. Thus it is not the optimum route all the way to ignition but it is certainly a promising approach to $Q \sim 1$.

Figure 8 shows the X-point results in the same plane. Evidently $Q \sim 0.1$ conditions are reached in the H-mode single null discharges even at 2MA (A Tanga, Kyoto, Nuclear Fusion etc.). These results were obtained with neutral beam heating only.

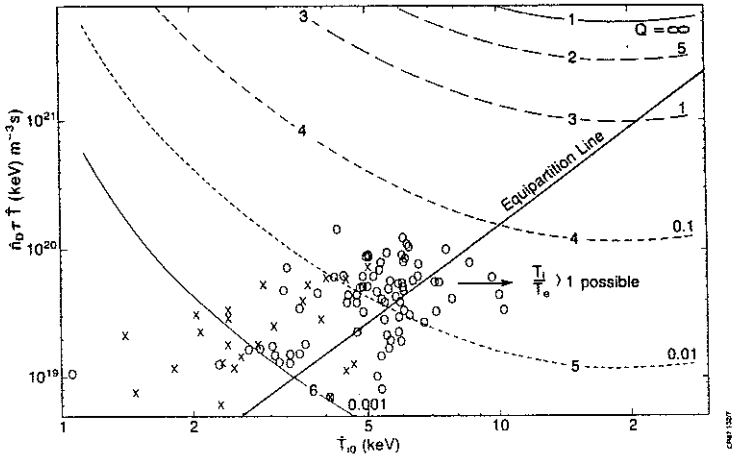

Fig. 8. Data for separatrix bounded plasmas, all heating schemes. X - Double null results (2MA), O Single null results (2&3MA). Upper single null results are H-modes all with only neutral beam heating. Contours of constant Q as in figures 4-7.

LIMITATIONS ON ADDITIONAL HEATING SYSTEMS

Neutral Beam Injection

The main limitations are on the plasma density. The density must be high enough to avoid excessive shine through and low enough to maintain a power deposition profile peaked in the central core of the plasma.

For JET with 120kV deuterium beams these limits are

$$1.10^{19}\text{cm}^{-3} < \bar{n} < 4\text{x}10^{19}\ \text{cms}^{-3}$$

Other factors notably limitations on confinement time mean that this is a fully acceptable operating range.

Ion Cyclotron Resonance Heating (ICRH)

ICRH has the proven advantage of very localised power deposition depending primarily on the choice of magnetic field, frequency and minority species. However there is a serious limitation due to the need to have the plasma boundary sufficiently close to the antenna screen in order to achieve good coupling. Figure 9 shows the theoretical and experimental variation of coupling resistance with plasma distance for the antennae used in the past. There is quite good agreement. Also shown are the theoretical values for the new design of antenna, eight of which are now installed on the machine. It is clear that it should be possible to couple significant power to the plasma in the promising scenario of X-point operation. In this case it is important that the plasma-antenna distance exceeds some critical value, at present unknown but probably ≥5cms. The importance of increasing the voltage hold-off capability of the antenna-feeder combination is also evident.

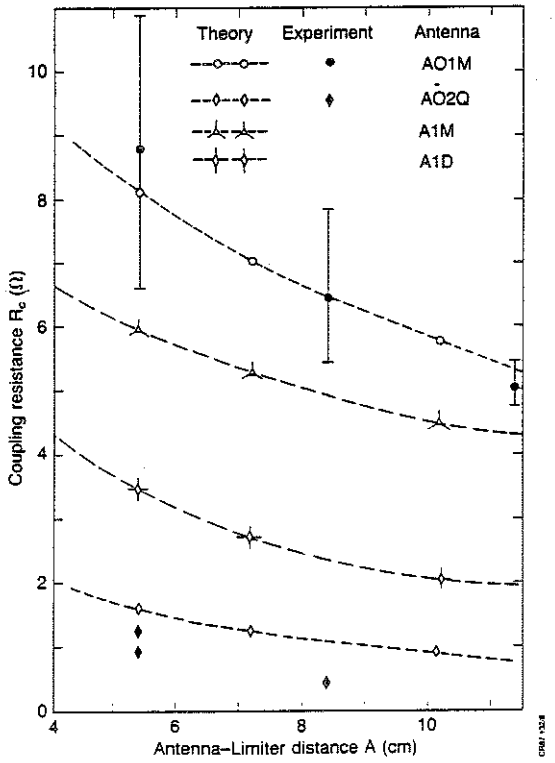

Fig. 9. Variation of coupling resistance R_c with antenna - plasma distance. A01M and A02Q are the antennae used in the 1985/1986 campaign in the monopole and quadrupole configurations. A1M and A1D are the newly installed antennae of different design operating in the monopole and dipole configurations. Coupled power is proportional to V^2R_c where V is the voltage on the antenna. A1D should have the same favourable properties as A02Q in that it has no component with $K_{\parallel}$ =0. At the same time it should have a higher coupling resistance.

β - Limits

The theory of limiting β due to MHD instabilities (Troyon et al, 1984) has been remarkably successful in predicting the operating limits which are observed experimentally. The Troyon limit is,

$$\bar{\beta} = 2.8 \frac{I}{Ba} \quad \% \qquad (\bar{\beta} \text{ is the value of } \beta \text{ averaged over the plasma volume})$$

and is derived by optimising the pressure profile. Hender et al (1987) have studied the MHD stability of a wider range of pressure profiles. For JET at 7MA and full field 3.5T they find the limits on $\bar{\beta}$ and β_o vs $P_o/\langle p \rangle$ shown in Fig. 10 for a given q_Ψ profile with q_Ψ=3.6 at the boundary. Evidently the more peaked the pressure profile the lower the permissible values of both β_o and $\bar{\beta}$ in this case. The thermonuclear Q depends very weakly on this profile provided $7<T_i<20$keV but depends linearly on central values of $\hat{n}\,\hat{T}_i\,\tau_e$, ie on $\beta_o\,\tau_E$. For JET with B=3.5T a thermonuclear Q=1 requires $\beta_o\tau_E$=9%s. Taking the maximum β_o from Hender et al (=15%) gives a simple requirement on τ_E, τ_E>0.6s for a profile in which $P_o/\langle p \rangle$ = 3.

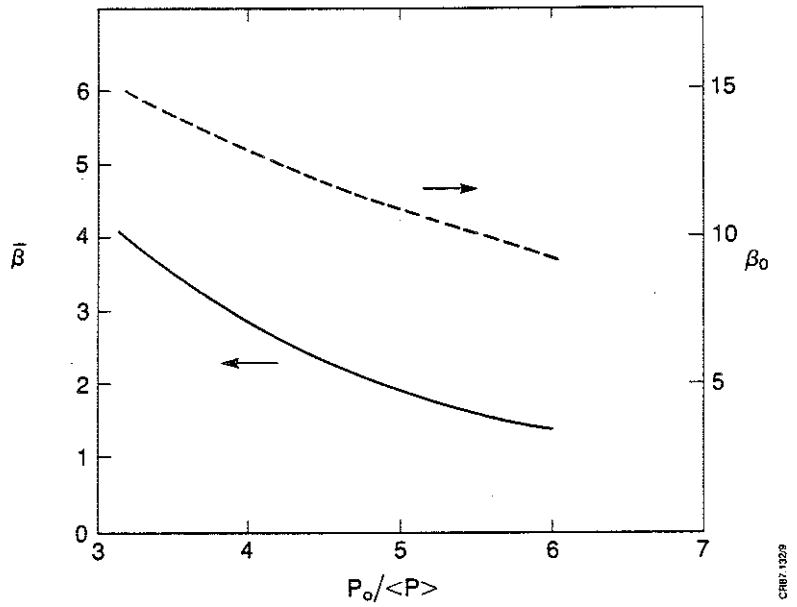

Fig. 10. Variation of ideal MHD stable values of $\bar{\beta}$ and β_o with the pressure peaking factor $p_o/\langle p \rangle$. Calculation is for q_Ψ ranging from 1.2 on the axis to 3.6 at the boundary corresponding to 7MA in JET with B_T=3.5T.

In Fig. 11 the present experimental results on $\bar{\beta}$ are plotted vs $I/_{Ba}$. The line represents the Troyon limit. Evidently we have achieved ∿ 0.6 x the limit in H-modes at currents of 2-3MA. As we will see later the combination of available input power and confinement time degradation is likely to be more limiting to JET performance than MHD modes.

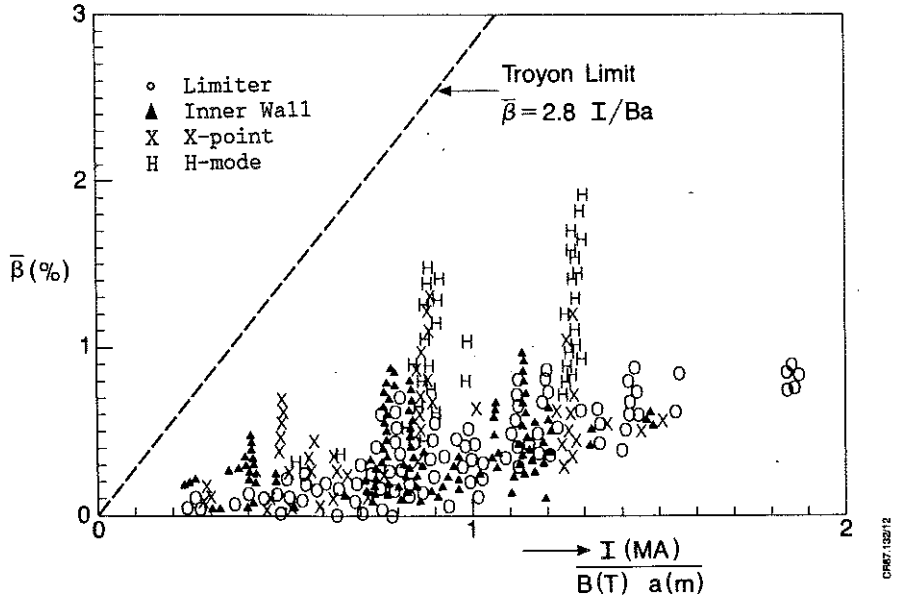

Fig. 11. The values of $\bar{\beta}$ derived from diamagnetic data versus the parameter I/Ba. Dotted line shows Troyon limit with K_T=2.8

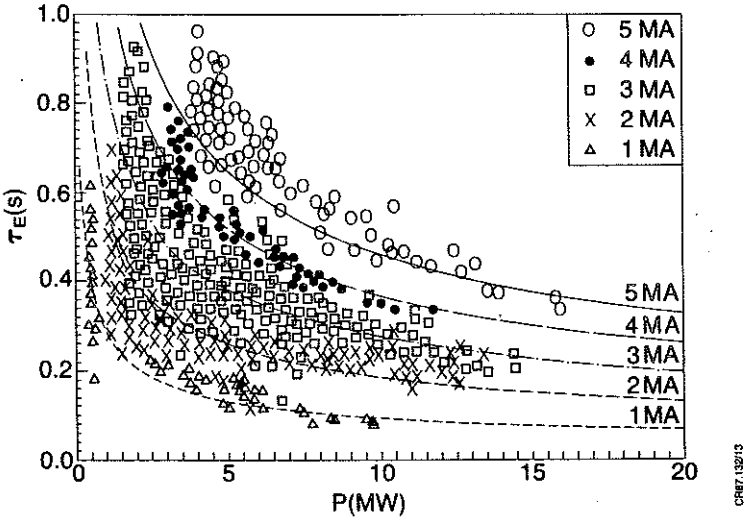

Fig. 12a. Confinement time τ_E versus input power for plasmas bounded on the inner wall or outer limiters. Lines are the predictions of the Goldston L-mode formula for an elongation of 1.4.

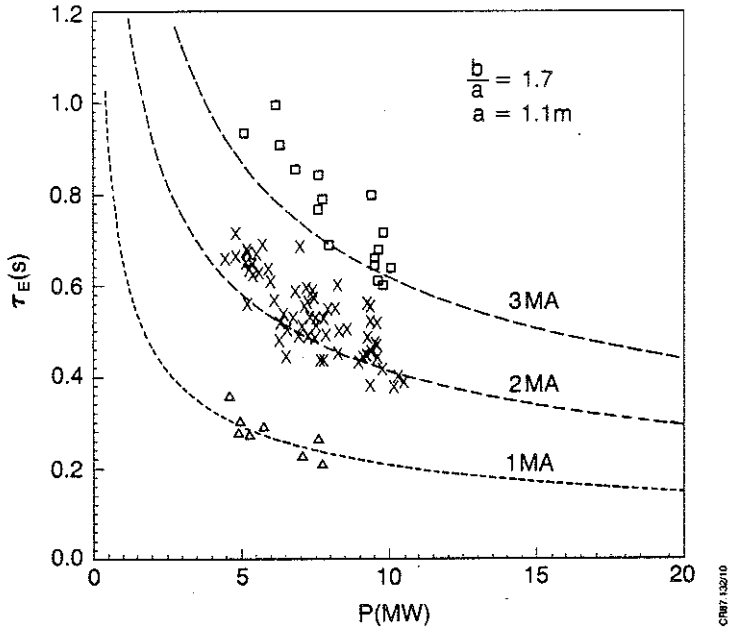

Fig. 12b. Confinement time versus input power for H-mode discharges with single null magnetic separatrix boundary. Lines are 2 x the predictions of Goldston L-mode scaling with the appropriate elongation. (=1.7)

ENERGY CONFINEMENT TIME

Figure 12a shows the confinement time vs power for all JET data excepting that for X-point operation. The lines plotted correspond to the scaling developed by Goldston (1984) namely,

$$\tau_E(s) = 3.7\times10^{-2}\ I_p\ P^{-\frac{1}{2}}\ R^{1.75}\ a^{-0.37}\ K^{\frac{1}{2}}$$

It is remarkable that this expression with unchanged constants fits JET data so well since it was derived from tokamaks smaller in physical scale by a factor 3 and smaller in maximum current by a factor 10.

The H-mode results (Tanga et al) show a similar degradation with power but an important improvement over the L-mode by just over a factor 2 as shown in Fig. 12b. These discharges do not reach a steady state, the density rises continuously so that the beam power is progressively deposited in the outer regions. Consequently the degradation of confinement time may not be an intrinsic feature of JET H-modes. (Keilhacker - this conference)

P. Thomas (1987) has used Connor-Taylor variables to derive a power law scaling fitting the JET data, for limiter discharges he finds

$$\tau_E(s) = 3.4\ (\tau_R\ \tau_A)^{0.5}\ \beta_I^{-1}$$

where τ_R is the resistive penetration time, τ_A the poloidal Alfven transit time and $\beta_I=(\frac{1+\varepsilon^2}{2\varepsilon}).\frac{2.12W}{I^2R}$ where W is the plasma energy content. (MJ).

Guided by a model in which a critical electron temperature gradient exists for the development of magnetic islands embedded in regions of stochastic field Rebut et al (1987) have derived an expression for the electron energy content of the plasma W_e,

$$W_e = \alpha_1\ Z^{\frac{1}{4}}\ n_e^{\frac{3}{4}}\ B^{\frac{1}{2}}\ I^{\frac{1}{2}}\ \ell''^{/4}\ (1+\alpha_2 \frac{M_i^{\frac{1}{2}} P}{n_e^{\frac{1}{2}}\ Z^{\frac{1}{2}}\ B\ell^{3/2}})^{\frac{1}{2}}$$

with $\alpha_1 = 2.3\times10^{-2}$, $\alpha_2 = 3$, $\ell = (abR)^{1/3}$ and units MJ, MA, MW, T, m, $10^{19}m^{-3}$

These three formulations show $\tau_E \propto P^{-\frac{1}{2}}$ at high power, they differ mainly in the dependence on n and I. Callen et al (1987) have analysed JET data in detail considering a balance between an inward

heat pinch and outward thermal conduction. They find an offset linear variation for the plasma stored energy versus input power. For high input power this leads to,

$$\tau_E(s) = 0.12\eta\ I$$

where η is a heating effectiveness which is a defined function of the power deposition and thermal diffusivity profiles. For typical present JET cases η=0.45 giving

$$\tau_E = 0.05\ I$$

For the expected JET parameters I_p=7MA, B=3.4T, a=1.2m, b=1.9m, P=40MW, $\bar{n}$=5x10^{19}m^{-3} the predictions for τ_E are,

Goldston L - mode	0.33s
Thomas model	0.43s
Rebut et al model	0.37s
Callen et al	0.32s

As might be expected for the relatively small extrapolation from present experiments the results do not differ very much. However since $Q \propto P\ \tau_E^2$ the predicted Q values will show more variation.

PERFORMANCE AND DEVICE EXTRAPOLATION

For the purpose of extrapolation we use the L-mode expression and characterise τ_E as $\tau_E = \gamma_g\ \tau_{EL}$ where τ_{EL} is the L-mode value. The central fusion parameter $X=\hat{n}\ \hat{T}\ \tau_E$ is then given by

$$X = 3.33 \times 10^{18}\ \frac{\gamma_n\gamma_T\gamma_g^2\ a^{1.26}\ R^{0.5}\ \varepsilon^2\ B^2}{q^2} \qquad (m^{-3},\ keV,s)$$

$$\gamma_n = \frac{\hat{n}}{\bar{n}}\ ,\ \gamma_T = \frac{\hat{T}}{\bar{T}}$$

This expression shows that X is a fixed characteristic of the device with the only possible variations through the γ values.

If we combine the L-mode scaling with the Troyon β limit then there is a condition on the heating power required,

$$P_1 = \frac{10.5\ a^{2.74}\ \varepsilon\ B^2\ K_T^2}{\gamma_g^2\ R^{1.5}} \qquad MW$$

where $\bar{\beta} = K_T\ I/B_a$ is used as the Troyon limit.

Combining the L-mode scaling with the Murakami parameter M gives a different condition on the power required,

$$P_2 = \frac{30\ M^2\ a^{0.74}\ q^2}{\gamma_g^2\ R^{1.5}\ \varepsilon}\ \left(\frac{\bar{T}}{10}\right)^2 \quad MW$$

where $\bar{T}$ is the average temperature (keV)

From these formulae with P for JET fixed at 40MW, q=1.8, $\gamma_n\gamma_T$=3, $\bar{T}$=5keV, we find

$$X = 2\times10^{20}\ \gamma_g^2$$
$$K_T = 0.8\ \gamma_g$$
$$M = 3.4\ \gamma_g$$
$$Q = 0.2\ \gamma_g^2$$

Since K_T<<2.8 we see that JET is confinement rather than β limited, that for γ_g=1, X $\sim$ 2x10^{20} correspond to Q $\sim$ 0.2 and that to reach this performance the tokamak must be operated with a relatively low value of M corresponding to $\bar{n}_e \sim 4\times10^{19}$m^{-3}. For the H-mode with γ_g=2 the predictions for 40MW input are

	I_p = 4MA	I_p = 6MA
X	2.6×10^{20}	6×10^{20}
K_T	1.6	1.6
M	3.4	5.0
Q	0.26	0.6

Since $K_T < 2.8$ it is clear that the normal critical β is not exceeded.

If we apply these expressions to the parameters of 'enhanced NET' (Engelmann, 1986) we find for the parameters, R=5.4m, a=1.7m, ε=2.2, B=4.8T, I=14.8MA a consistent set for ignition with $X = 5 \times 10^{21} m^{-3}$ keV seconds, P=100MW, τ_E=2.8s, $p/\bar{p}$=3, γ_g=2.2 (requiring H-mode) $\bar{n} = 7 \times 10^{19} m^{-3}$ (M=8). These figures are all plausible on the basis of the present JET data. The Rebut-Lallia scaling is more pessimistic and requires an H-mode type improvement of $\sim$ 2.5 in the confinement time for ignition. Callen-Cordey scaling, assuming a $(\text{size})^2$ dependence is more optimistic and predicts ignition without an H-mode improvement.

NON THERMAL CONTRIBUTIONS TO Q

With neutral beam heating we can expect contributions to Q due to reacting collisions between the fast beam ions themselves Q_{bb} and between beam and background 'plasma' ions, Q_{bp}. The contribution due to Q_{bb} is dominant at low plasma densities and high input power since

$$Q_{bb} \propto \frac{P_b \, \varepsilon_b}{n_e^2} \quad \frac{1}{\text{volume}}$$

while $Q_{b-p} \propto \varepsilon_b^{1/2}$ where ε_b is the energy of the injected beam ions.

This is for the case where $\varepsilon_b < \varepsilon_c$ the critical energy ($\sim 20 T_e$) below which the fast ions slow down by collisions with background ions. Figure 13 shows the predicted Q values with 20MW of RF, 20MW of NBI and confinement times in the range extrapolated from present experiments. Evidently the maximum total Q is achieved at low density and contains a significant non-thermal contribution.

Taking into account the earlier evidence on confinement time we see that it should be possible to achieve a total Q $\sim$ 1 in 7MA limiter or 4MA X-point operation. With 6MA X-point operation total Q $\sim$ 1.5 should be possible.

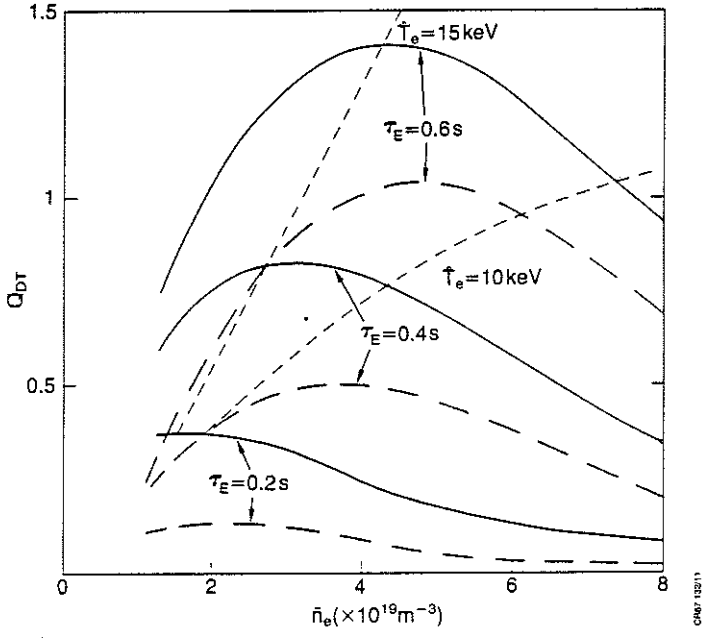

Fig. 13. Predicted Q values for various values of confinement time. Power input is 20MW ICRH and 20MW neutral beam injection. Dashed lines show thermonuclear Q. Continuous lines show total Q values including beam plasma contributions. (1.1 D-T mixture without depletion)

CONCLUSIONS

(a) JET operation is limited in the normalised density vs normalised current plane in much the same way as all other tokamaks but with a maximum Murakami parameter ~ 6 at $1/q_{CYL} \sim 0.6$. High density disruptions are due to current channel shrinkage as the radiated power in the periphery rises.

(b) Conditions have been achieved in deuterium corresponding to a thermonuclear $Q \sim 0.07$ in a D-T mixture.

(c) JET performance has been well below the β-limit so far. It is likely to remain so with limiter operation but with higher current H-modes the Troyon limit may be approached.

(d) All JET operation shows severe confinement degradation as the heating power is increased.

(e) Different interpretations of the existing data lead to much the same predictions for operation at the extended parameters of current and power that will be used in the future.

(f) To achieve thermonuclear $Q \sim 1$ requires $\tau_E > 0.6$s due to the MHD stability limitations on β_o.

(g) A total $Q \sim 1.0$ is a realistic prediction when thermonuclear and beam-plasma contributions are included.

(h) The presently accessible values of M are fully adequate. Indeed with 40MW of input power the average density must be kept below $4 \times 10^{19} m^{-3}$ in order to get a high enough average temperature.

(i) On the basis of present JET data a machine with the parameters of 'enhanced NET' should ignite provided H-mode type confinement is achieved.

REFERENCES

Callen, J. D., J. P. Christiansen, J. G. Cordey, P. R. Thomas and K. Thomsen (1987). JET Preprint - P(87)10.

Campbell, D. J. et al (1986). 11th International Conference on Plasma Physics & Controlled Nuclear Fusion Research, Kyoto, IAEA-CN-47/A-VII-5.

Engelmann, F. (1986). NET Report. EUR-FUI/XII - 80/86/64.

Goldston R. (1984). Plasma Physics & Controlled Fusion, 26, 87.

Hender, T. C., P. S. Haynes, D. C. Robinson and A. Sykes (1987). Proceedings 13th EPS Conference on Controlled Fusion & Plasma Physics, Madrid.

Keilhacker, M. (1987). Proceedings 13th EPS Conference on Controlled Fusion and Plasma Physics, Madrid.

Rebut, P. H. and P. P. Lallia (1987). 7th International Conference on Plasma Physics, Kiev.

Snipes J. et al (1987) Proceedings 13th EPS Conference on Controlled Fusion & Plamsa Physics, Madrid.

Tanga, A. et al (1986). 11th International Conference on Plasma Physics and Controlled Nuclear Fusion Research, Kyoto, IAEA-CN-47/K-I-1.

Thomas P. Resistive MHD Scaling paper. JET Preprint P-(87)17.

Troyon F., R. Gruber, H. Sauremann, S. Semenzato and S. Succi (1984). Plasma Physics & Controlled Fusion, 26, 209.

APPENDIX I

THE JET TEAM

JET Joint Undertaking, Abingdon, Oxon, OX14 3EA, U.K.

J. M. Adams[1], H. Altmann, R. J. Anderson, D. V. Bartlett, W. Bailey, K. Behringer, E. Bertolini, P. Bertoldi, C. H. Best, V. Bhatnagar[2], R. J. Bickerton, A. Boileau[3], T. Bonicelli, S. J. Booth, A. Boschi, G. Bosia, M. Botman, G. Bracco[4], H. Brelen, H. Brinkschulte, M. L. Browne, M. Brusati, T. Budd, M. Bures, H. Buttgereit, D. Cacaut, C. Caldwell-Nichols, J. Callen[5], D. J. Campbell, J. Carwardine, G. Celentano, C. D. Challis, A. Cheetham, J. Christiansen, C. Christodoulopoulos, P. Chuilon, R. Claesen, J. P. Coad, S. Cohen[6], S. Conroy[14], M. Cooke, J. G. Cordey, W. Core, S. Corti, A. E. Costley, G. Cottrell, M. Cox[7], P. Cripwell[14], D. Cross, C. David[18], E. Deksnis, A. de Matteis[8], J. Deng[9], G. B. Denne, G. Deschamps, K. J. Dietz, J. Dobbing, S. E. Dorling, D. F. Düchs, G. Duesing, P. Duperrex[10], H. Duquenoy, L. de Kock, A. Edwards, J. Ehrenberg[15], W. Engelhardt, S. K. Erents[7], B. T. Eriksson, H. Falter, M. Forrest[7], C. Froger, K. Fullard, M. Gadeberg[11], A. Galetsas, A. Gibson, R. D. Gill, A. Goede, A. Gondhalekar, G. Gorini, C. Gormezano, N. A. Gottardi, C. Gowers, R. Granetz, B. J. Green, F. S. Griph, R. Haange, J. H. Hamnén[12], C. J. Hancock, P. J. Harbour, P. Haynes[7], T. Hellsten, J. L. Hemmerich, R. Hemsworth, F. Hendriks, R. F. Herzog, K. Hirsch[15], J. Hoekzema, L. Horton[13], J. How, M. Huart, A. Hubbard[14], M. Hugon, M. Huguet, B. Ingram, H. Jäckel[15], J. Jacquinot, Z. Jankowicz[16], O. N. Jarvis, E. Joffrin, E. M. Jones, T. T. C. Jones, P. D. Jones, E. Källne, J. Källne, A. Kaye, B. E. Keen, M. Keilhacker, S. Knowlton, A. Konstantellos, M. Kovanen[22], P. Kupschus, P. Lallia, J. R. Last, L. Lauro-Taroni, E. Lazzaro, R. C. Lobel, P. Lomas, N. Lopes-Cardozo[17], M. Lorentz-Gottardi, C. Lowry[14], G. Magyar, D. Maisonnier, M. Malacarne, V. Marchese, P. Massmann, G. McCracken[7], M. J. Mead, P. Meriguet, S. F. Mills, P. Millward, A. Moissonnier, P. L. Mondino, D. Moreau[18], P. Morgan, H. Morsi[15], G. Murphy, M. F. Nave, L. Nickesson, P. Nielsen, P. Noll, S. Nowak, W. Obert, D. O'Brien, K. Odajima[19], J. O'Rourke, T. Oyevaar[17], M. G. Pacco, J. Paillere, M. Pain, S. Papastergiou, D. Pasini[21], M. Paume, N. Peacock[7], M. Pick, J. Plancoulaine, J-P. Poffé, R. Prentice, T. Raimondi, J. Ramette[18], C. Raymond, P. H. Rebut, J. Removille, W. Riediker, F. Rimini, D. Robinson[11], A. Rolfe, R. T. Ross, G. Rupprecht[15], R. Rushton, H. C. Sack, G. Sadler, J. Saffert, N. Salmon[14], H. Salzmann[15], A. Santagiustina, M. Schmid, F. C. Schüller, K. Selin, R. L. Shaw, K. Shibonuma[19], R. Sillen[17], R. Simonini, P. Smeulders, J. Snipes, L. Sonnerup, K. Sonnenberg, M. Stamp, P. Stangeby[20], D. Start, C. A. Steed, D. Stork, P. E. Stott, T. E. Stringer, D. Summers, H. Summers[21], J. Tagle, H. Tamnen, A. Tanga, A. Taroni, A. Tesini, P. R. Thomas, E. Thompson, K. Thomsen[11], F. Tibone, P. Trevalion, M. Tschudin, B. Tubbing[17], E. Usselmann, H. van der Beken, M. von Hellermann, J. E. van Montfoort, T. Wade, C. Walker, B. A. Wallander, M. Walravens, K. Walter, D. Ward, M. L. Watkins, M. Watson, J. Wesson, E. Westerhoff[15], J. Wilks, T. Winkel, C. Woodward, M. Wykes, D. Young, L. Zannelli, J. W. Zwart

PERMANENT ADDRESS

[1] UKAEA, Harwell, Nr. Didcot, Oxon, UK.
[2] EUR-EB Association, LPP-ERM/KMS, B-1040 Brussels, Belgium.
[3] Institute National des Recherches Scientifique, Quebec, Canada.
[4] ENEA-CENTRO Di Frascati, I-00044 Frascati, Roma, Italy.
[5] Dept. of Physics, University of Wisconsin, Madison, U.S.A.
[6] Princeton Plasma Physics Laboratory, New Jersey, U.S.A.
[7] UKAEA Culham Laboratory, Abingdon, Oxfordshire, U.K.
[8] ENEA-CRE, Bologna, Italy.
[9] IPP, Hefei, China,
[10] CRPP/EPFL, 21 Avenue des Bains, CH-1007 Lausanne, Switzerland.
[11] Risø National Laboratory, DK-4000 Roskilde, Denmark.
[12] Swedish Energy Research Commission, S-10072 Stockholm, Sweden.
[13] Natural Sciences and Engineering Research Council, Ottawa, Canada.
[14] Imperial College of Science and Technology, University of London, U.K.
[15] Max Planck Institut für Plasmaphysik, D-8046 Garching bei Munchen, F.R.G.
[16] Institute for Nuclear Studies, Swierk, Poland.
[17] FOM Instituut voor Plasmafysica, 3430 Be Nieuwegein, The Netherlands.
[18] Commissariat a L'Energie Atomique, F-92260 Fontenay-Aux-Roses, France.
[19] JAERI, Tokai Research Establishment, Tokai-Mura, Naka-Gun, Japan.
[20] Institute for Aerospace Studies, University of Toronto, Downsview, Ontario, Canada.
[21] University of Strathclyde, 107 Rottenrow, Glasgow, U.K.
[22] Dept. of Physics, Lapeenranta University, Finland.